Infrared optical response of LuFe_{2}O_{4} under dc electric field

Chul Lee, JooYoun Kim, S. W. Cheong, and E. J. Choi

Phys. Rev. B **85**, 014303 — Published 25 January 2012

DOI: 10.1103/PhysRevB.85.014303

Infrared-Optical response of $LuFe_2O_4$ under dc-Electric field

Chul Lee[1], JooYoun Kim[1], S. W. Cheong[2] and E. J. Choi[1]
[1] *Department of Physics, University of Seoul, Seoul 130-743, Republic of Korea and*
[2] *Rutgers Center for Emergent Materials & Department of Physics and Astronomy, Rutgers University, Piscataway, New Jersey 08854, USA*

We applied dc-voltage (V) to $LuFe_2O_4$ single crystal and measured the V-dependent optical reflectivity. As V increases an optical absorption band appears at mid-infrared frequency range which we could identify to result from the dc-electric (E) field. We discuss possible connection of this novel electro-optical effect with the strongly correlated states in $LuFe_2O_4$. In the mean time a reflectivity level change is seen in the IR $\sim$ visible frequency range by the V-application due to the Joule heating of the sample.

PACS numbers: 78.30.Hv, 75.25.Dk, 63.20.-e

I. INTRODUCTION

The mixed-valent compound $LuFe_2O_4$ has drawn attention recently since the discovery of ferroelectricity with the electronic origin. The unit cell of $LuFe_2O_4$ exhibits double-layer structure consisting of alternatively stacked Fe-O planes. While the Fe-ions have the mixed valency $Fe^{2.5+}$ at high temperature, they undergo the Verwey-type transition at $T_{CO} = 320$ K in which the charge-ordered Fe^{2+}- and Fe^{3+}- sublattices are formed. In the charge-ordered state the centers of the Fe^{2+}- and Fe^{3+}- sublattices do not coincide and consequently finite electrical polarization is induced which leads to the emergence of the bulk ferroelectric phase.[1] This phenomenon, termed as the "electronic-ferroelectricity", is distinguished from the traditional ferroelectricity where the electric polarization is induced by the displacement of charged ions as known in, for example, $BaTiO_3$. As temperature decreases the localized spins of the Fe^{2+} and Fe^{3+} show the ferrimagnetic ordering at $T_N = 240$ K. The ferroelectricity and the magnetism are coupled with each other as revealed by recent X-ray scattering experiment.[2] A large magneto-dielectric change was observed[3] which indicates the presence of multiferroic effect in this compound.

Optical property of $LuFe_2O_4$(LFO) has been studied by a few groups until now: Xu *et al.* observed the optical absorption peaks due to the charge-transfer excitation between the ions, i.e, between O^{2-} and $Fe^{2.5+}$ (Lu^{3+}), and between Fe^{2+} and Fe^{3+}.[4] Vitucci *et al.* measured the optical phonon spectrum at the Far-infrared frequency and studied how the phonon frequency and intensity change at the charge ordering transition.[5] In time-domain spectroscopy of LFO, some sub-terahertz excitation modes were detected.[6] In this work we applied the dc-voltage (V) to LFO crystal and measured subsequent voltaic effect on the optical reflectivity spectrum. The dc-electric field (dc E-field) applied to a solid often leads to novel optical response. For example Anastassakis *et al.* discovered that in the diamond crystal a sharp infrared absorption shows up when dc-V is turned on.[7] In general context the dc E-field displaces the charge and lattice from their equilibrium positions, consequently inducing finite dipole moment and also breaking the symmetry of the solid. Optical radiation incident on the solid can couple with the induced dipole moment and excite optical resonance which was symmetry-forbidden by the selection rule in the high-symmetry state before the dc E-field was applied. In the experiment of Ref. 7 on the diamond, the sharp IR peak was interpreted as a Raman phonon mode which was inactive in the IR spectrum at E = 0.[8] Noting that LFO exhibits the rich phases due to the strong correlation effect –charge ordering, ferroelectricity, and the magnetism– that diamond is lacking, one may expect that the dc E-field by interacting with the charge, dipole moment, and the spin of LFO can induce new optical excitation(s) in the optical response. To put the result upfront we indeed find an optical absorption band activated by the dc-E. This E-induced absorption is, however, notably different from that in diamond in several aspects as to be discussed later.

The effect of dc-voltage on the transport property of LFO was studied previously by Li *et al.* There some changes in the dc-resistance[9] and in the bulk magnetization[10] were seen by the application of dc-V which was interpreted in terms of the dc E-field breaking or melting the charge-ordered state. However Wen *et al.* showed, based on their neutron scattering experiment, that the charge-ordered state and the spin-ordered state in LFO are not destroyed by the dc-voltage.[11] Instead they proposed that the changes observed in Ref. 9 and Ref. 10 are due to the rise of sample temperature caused by the dc-V driven current flow, i.e, the Joule heating. This controversy, which partly motivated us to perform the present optical study, shows that the E-field effect and the Joule heating effect should be carefully measured and interpreted separately in any dc V-driven experiment. Having said that we fulfill the requirement in this work by performing the V-driven measurement of optical reflectivity as well as an independent T-driven measurement in which the optical reflectivity is measured at elevated temperature but without applying the dc-voltage. By comparing the two sets of the experimental data, the V-driven and the T-driven optical responses, we were able to identify the non-trivial dc E-field induced optical effect in LFO aside from the less-interesting, Joule heating-induced effect.

II. EXPERIMENT

$LuFe_2O_4$ single crystal was grown by the floating zone method. The LFO crystal, 5.6 mm × 3.5 mm in area and 1 mm thick, was glued on thin sapphire substrate and the LFO/sapphire composite was mounted on temperature-variable optical cryostat. The optical reflectance was measured on the large surface of the sample which contains the c- and a(or b)-axis. In the dc-V application experiment the voltage was applied on the two small surfaces of the sample which creates the dc-electric field along the long (5.6 mm) c-axis ($\mathbf{E}//\mathbf{c}$). The Joule-heat caused by the current flow in the sample was efficiently drawn out to the thermal bath with the aid of the high thermal conductivity of the sapphire base which consequently minimized the unwanted rise of the sample temperature. In the T-driven experiment the temperature of the sample (and the sapphire) was controlled using the heating coils mounted in the optical cryostat. The normal-incident and unpolarized optical reflectance was measured using a Fourier transform interferrometor (FTIR) over the Far-IR ∼ visible frequency region (150 ∼ 10000 cm^{-1}). In the dc-V experiment we first took the reflectance at zero voltage (= R(0)) and continued subsequent reflectance measurement with the dc-V applied on the sample (= R(V)) without moving the sample position. From R(V) and R(0) the normalized reflectance R(V)/R(0) was calculated which we will present in this paper. At V = 0, we also measured the *absolute* reflectivity $R_{abs}(\omega)$ for the quantitative analysis of data as to be described later.

III. RESULTS AND DISCUSSIONS

Fig.1 shows the relative reflectivity R(V)/R(0) measured for the dc-voltage in $0 \leq V \leq 7$ V range. As dc-V is applied the level of the R(V)/R(0) curve decreases in the infrared and visible frequency region. The sharp features at low frequency $\omega < 1000$ cm^{-1} are due to optical phonons of LFO which we will discuss in detail in Fig. 2. The dc-V creates the dc-electric field and the Joule heat in the sample simultaneously. To identify the optical change by the Joule heat we measured the reflectivity with the dc-V turned off and instead increasing the sample temperature to obtain the relative spectra R(T)/R(0) for 290 K(RT) $\leq$ T $\leq$ 380 K. Here R(0) represents the reflectance measured at room-temperature and at V = 0. The measured R(T)/R(0) showed the same behavior (Figure not shown) as R(V)/R(0), i.e, the decrease of the reflectance level over the wide frequency range with increasing T. It indicates that the observed V-driven optical change is caused by the Joule heating. However an interesting behavior is observed at low frequency in R(V)/R(0). Fig. 2(a) and (b) display the dc-V-driven change R(V)/R(0) and the temperature-driven change R(T)/R(0) respectively in the Far-infrared region 150 $cm^{-1} < \omega < 1000$ cm^{-1}. At $\omega > 700$ cm^{-1} a hump structure appears in R(V)/R(0). This clear and well-defined feature is however absent in R(T)/R(0). The hump feature is therefore assigned unarguably as a non-thermal effect which is free from the Joule heating. At $\omega < 700$ cm^{-1} the two sets of data R(V)/R(0) and R(T)/R(0) exhibit again similar behaviors.

To understand the origin of the V-driven hump we will calculate the optical conductivity function $\sigma(\omega)$. $\sigma(\omega)$ is obtained from the Kramers-Kronig transformation of the absolute reflectivity spectrum. As first step toward $\sigma(\omega)$ we measured the absolute reflectivity of LFO at V = 0, $R_{abs}(0) = R(0)/R_{Au}$, where R_{Au} is the reference reflectance of Au-film. Then we calculate $[R(V)/R(0)]\cdot R_{abs}(0)$ which is reduced to $R(V)/R_{Au} = R_{abs}(V)$, the absolute reflectivity at finite dc-V. We performed the same calculations for the T-driven data to obtain $R_{abs}(T) = [R(T)/R(0)]\cdot R_{abs}(0)$, the absolute reflectivity at the elevated temperatures. Fig. 3 depicts the $R_{abs}(V)$ and $R_{abs}(T)$ in the panel (a) and (b) respectively. They both show the optical phonon structure of LFO at $\omega < 700$ cm^{-1}. The intensity of $R_{abs}(V)$ decreases slightly as V increases which is also seen in $R_{abs}(T)$ as T increases. The inset of (a) shows the behavior of the V-driven hump closely in the expanded scale. At V = 0 the hump is absent whereas it grows as V is applied. Note that the absolute intensity of the hump in $R_{abs}(V)$ is much weaker than the intensity of the optical phonons unlike in the relative reflectance R(V)/R(0) of Fig. 2 in which the hump had the comparable strength as those of the phonons. It is due to that the reflectivity level of $R_{abs}(0)$ is significantly lower at the frequency of the hump than that in the phonon region. Now we apply the Kramers-Kroning (KK) transformation on $R_{abs}(V)$ and $R_{abs}(T)$. For the KK analysis, we employ the constant-R extrapolation in the low frequency limit $\omega \rightarrow 0$. In the high-frequency limit the absolute reflectivity was extended up to 50000 cm^{-1} above which free-electron approximation $R_{abs} \sim \omega^{-4}$ was assumed. The constant-R extrapolation at the low frequency limit brings about some uncertainty in $\sigma(\omega)$ which however does not affect the optical conductivity in the region of the hump. We also calculated $\sigma(\omega)$ using the variational dielectric function (VDF) algorithm developed by A. Kuzmenko[12], to find that the V- and T- dependent optical conductivity are identical to those obtained from the KK-transformation.

Fig. 4(a) and (b) display $\sigma_1(\omega)$, the real part of the $\sigma(\omega)$ spectrum, for the V-driven and T-driven experiment respectively. In (a) the phonon peak height decreases gradually as V is applied. For the phonon mode at $\omega = 550$ cm^{-1} the peak position shifts to lower frequency with increasing V. The phonon shift is seen in the T-driven $\sigma_1(\omega)$ as well indicating that the shift in (a) is due to the Joule heating.[13] We make use of this observation to estimate the sample temperature in the V-driven measurement. For example note that the intensity of $\sigma_1(\omega)$ and the phonon position at V = 7 volt is very close to those of $\sigma_1(\omega)$ at T = 340 K, which enables us determine the rise of sample temperature by ∼ 50 K from the room-temperature 290 K at this dc-voltage. The two insets again show $\sigma_1(\omega)$ closely in the region

of the hump. With the two sets of optical conductivity $\sigma_1(V)$ and $\sigma_1(T)$ we proceed to calculate the conductivity difference $\Delta\sigma_1(V) = \sigma_1(V)$ - $\sigma_1(0)$ and $\Delta\sigma_1(T) = \sigma_1(T)$ - $\sigma_1(0)$. The V-driven and T-driven conductivity difference are shown in Fig. 5(a) and Fig. 5(b) respectively. One can decompose the V-driven difference $\Delta\sigma_1(V)$ into two parts, (1) the dc-E field induced effect and (2) the effect due to the Joule heating. We express therefore $\Delta\sigma_1(V)$ as $\Delta\sigma_1(V) = \Delta\sigma_1(T) + \Delta\sigma_1(\mathrm{E})$ and extract the E-field term $\Delta\sigma_1(\mathrm{E})$ by removing $\Delta\sigma_1(T)$ from $\Delta\sigma_1(V)$ as $\Delta\sigma_1(\mathrm{E}) = \Delta\sigma_1(V)$ - $\Delta\sigma_1(T)$. In the substraction $\Delta\sigma_1(V)$ - $\Delta\sigma_1(T)$ we used T = 340 K for V = 7 V and T = 320 K for 6.5 V and 6 V as the sample temperature. This T-assignment is based on the peak position shift of the 560 cm^{-1}-phonon in the V-driven $\sigma_1(V)$ and the T-driven $\sigma_1(T)$. To check the T-assignment we independently estimate the dc-V induced temperature rise ΔT using the heat diffusion equation $\mathrm{P}\cdot\mathrm{dt} = \mathrm{c}\cdot\mathrm{m}(\partial\mathrm{T}/\partial\mathrm{t})\mathrm{dt} + \mathrm{k}[\mathrm{T(t)} - \mathrm{T}_0]\mathrm{dt}$. Here the first term is the energy input from the heater ($\mathrm{P} = \mathrm{I}\cdot\mathrm{V}$), the second term being the increase of sample temperature in which c and m are the heat capacity and mass of the sample respectively. The last term represents the leak of energy to the surrounding bath through the sapphire base where k is the heat conductivity of Al_2O_3 (= 30 W/mol·K) and T(t) - T_0 is the temperature difference between the sample (= T(t)) and the bath (T_0 = 290 K) respectively. This equation leads to $\Delta\mathrm{T} = (\mathrm{P/k})$ at equilibrium. Under our experimental condition (V = 7 V, I = 1 A) we obtain Δ T= 58 K which is close to ΔT = 50 K estimated from the phonon shift. The result of the conductivity subtraction is shown in Fig. 5(c). $\Delta\sigma_1(\mathrm{E})$, the purely E-field induced change, exhibits an hump with the rapid increase at ω = 700 cm^{-1} and slow-decay at high-ω. This behavior of $\Delta\sigma_1(\mathrm{E})$ is notably different from the E-induced IR peak observed in diamond. In the dc-V experiment on diamond the IR peak that appeared at ω = 1332.6 cm^{-1} had narrow peak width less than 5 cm^{-1} and the symmetric line shape.[7,8] In contrast the $\Delta\sigma_1(\mathrm{E})$ hump in LFO is very broad and should be considered as an absorption band rather than a peak. Also the $\Delta\sigma_1(\mathrm{E})$-band has strongly asymmetric shape. Such aspects point toward non-phonon origin of $\Delta\sigma_1(\mathrm{E})$.

A broad and asymmetric IR-band was observed in, among others, the anti-ferromagnetic (AF) cuprates such as La_2CuO_4, $Sr_2CuO_2Cl_2$ and CuO. There the asymmetric mid-IR band came from the magnetic-origin, i.e, the phonon-assisted two-magnon excitation of the Cu^{2+} spins (S = 1/2).[14–18] One may assume that similar excitation is occuring in $LuFe_2O_4$ and consider $\Delta\sigma_1(\mathrm{E})$ as the bi-magnon band. In the cuprates the two-magnon band persists even in the paramagnetic state $\mathrm{T} > \mathrm{T}_N$ due to the remaining short range spin order. Perhaps it will apply to LFO as well because the $\Delta\sigma_1(\mathrm{E})$-band is observed at T > 290 K although T_N is lower (240 K). In the cuprates the bi-magnon band is seen at E = 0 due to that the optical-phonon is exited by IR simultaneously with the bi-magnon. In contrast LFO requires the dc-E for the $\Delta\sigma_1(\mathrm{E})$-band to be activated in IR suggesting that IR couples to the localized spins through some different route. As another possible origin of the $\Delta\sigma_1(\mathrm{E})$-band we note that in weakly doped transition metal-oxide compounds optical absorption due to the lattice polaron is observed in the IR-frequency range. Here the carriers are bound to the lattice due to the electron-phonon interaction and forms the small- or the large-polarons. The polaron can absorb the photon and be excited into the higher energy states. This photo-ionization process results in a broad and asymmetric absorption band in the optical conductivity as seen in, for example, $La_{2-x}Sr_xCuO_{4+\delta}$, $La_{2-x}Sr_xNiO_{4+\delta}$, MgO and BeO.[19,20] Considering the natural carrier doping due to non-stoichiometry in LFO, it is reasonable to expect that the polaron absorption will be present in ionic crystal $LuFe_2O_4$ as well. D. Emin calculated the optical conductivity function $\sigma_1(\omega)$ due to the small and large polaron absorption process theoretically.[21] For the large polaron $\sigma_1(\omega)$ case, $\sigma_1(\omega)$ band increases rapidly at $\omega = \mathrm{E}_b$ (= polaron binding energy) and decays slowly at the high frequency side of the band. This predicted spectral shape is similar to the $\Delta\sigma_1(\mathrm{E})$-band of LFO. If we assign $\Delta\sigma_1(\mathrm{E})$ to the polaron band we are faced with the question that why or how it is induced by the E-field but not so by the temperature increase which we believe further study is needed answer.

At this point we could only suggest some possible scenarios for the origin of $\Delta\sigma_1(E)$ without firmly pinning it down. Nevertheless it is clear that the observed IR-band is truly an E-driven change which is rarely seen in solid. In the diamond crystal the IR-peak is activated by strong dc-electric field $\mathrm{E} \sim 10^5$ V/cm whereas in contrast the IR-band in LFO is induced at much lower field, E ~ 10 V/cm. It suggests again that the latter effect comes from some exotic mechanism different from that in diamond.

IV. CONCLUSION

In conclusion we have measured optical reflectance $\mathrm{R}(\omega)$ of $LuFe_2O_4$ crystal with dc-voltage applied on it. As dc-V is applied a broad and asymmetric optical absorption band is observed in $\sigma_1(\omega)$ at infrared frequency $\omega >$ 700 cm^{-1}. The IR-band is not seen in our independently performed T-driven reflectivity measurement in which the sample temperature was raised without applying the dc-V. This comparative study shows therefore that the IR-band is not due to the Joule-heating but is a purely dc-electric field induced effect. We compared this novel IR-absorption with the E-induced IR-peak in diamond crystal and conclude that the IR-band in LFO has non-phonon origin. We discussed possible sources of the dc-E field induced IR band in relation with the correlated phases of LFO such as the bi-magnon excitation and the polaron absorption band. Further study is encouraged to understand the exact origin of the low E-field activated IR-band. In particular microscopic theory on the effect of the dc-E field and the coupling of IR with the spin/charge/lattice in LFO is needed. Aside from the dc-E induced IR-band, we also showed that the

gradual decrease of R(ω) takes place over the Far-IR $\sim$ visible frequency range as result of the Joule-heating.

We thank K. H. Kim for useful discussions. This work was supported by Basic Science Research Program through NRF of Korea (Grant No. 2010-0008281) and National Nuclear Research and Development Program through the NRF of Korea (Grant No. 2010-0018559).

[1] N. Ikeda, H. Ohsumi, K. Ohwada, K. Ishii, T. Inami, K. Kakurai, Y. Murakami, K. Yoshii, S. Mori, Y. Horibe, and H. Kito, Nature (London) **436**, 1136 (2005).

[2] M. Angst, R. P. Hermann, A. D. Christianson, M. D. Lumsden, C. Lee, M.-H. Whangbo, J.-W. Kim, P. J. Ryan, S. E. Nagler, W. Tian, R. Jin, B. C. Sales, and D. Mandrus, Phys. Rev. Lett. **101**, 227601 (2008).

[3] M. A. Subramanian, Tao He, Jiazhong Chen, Nyrissa S. Rogado, Thomas G. Calvarese, and Arthur W. Sleight, Adv. Mater. **18**, 1737 (2006).

[4] X. S. Xu, M. Angst, T. V. Brinzari, R. P. Hermann, J. L. Musfeldt, A. D. Christianson, D. Mandrus, B. C. Sales, S. McGill, J.-W. Kim, and Z. Islam, Phys. Rev. Lett. **101**, 227602 (2008).

[5] F. M. Vitucci, A. Nucara, D. Nicoletti, Y. Sun, C. H. Li, J. C. Soret, U. Schade, and P. Calvani, Phys. Rev. B **81**, 195121 (2010).

[6] S. Z. Li, S. J. Luo, R. Fu, B. B. Jin, K. F. Wang, J.-M. Liu, J. F. Ding, and X. G. Li, J. Appl. Phys. **96**, 893 (2009).

[7] E.Anastassakis, and E. Burstrin, Phys. Rev. B **2**, 1952 (1970).

[8] E.Anastassakis, S. Iwasa, and E. Burstrin, Phys. Rev. Lett. **17**, 1051 (1970).

[9] Changhui Li, Xiangqun Zhang, Zhaohua Cheng, and Young Sun, Appl. Phys. Lett. **93**, 152103 (2008).

[10] Chang-Hui Li, Fen Wang, Yi Liu, Xiang-Qun Zhang, Zhao-Hua Cheng, and Young Sun, Phys. Rev. B **79**, 172412 (2009).

[11] Jinsheng Wen, Guangyong Xu, Genda Gu, and S. M. Shapiro, Phys. Rev. B **81**, 144121 (2010).

[12] A. B. Kuzmenko, Rev. Sci. Instrum. **76**, 083108 (2005).

[13] The previous IR-study in Ref. 5 also showed that the phonon peak shifts as the sample tempeature changes.

[14] J. D. Perkins, J. M. Graybeal, M. A. Kastner, R. J. Birgeneau, J. P. Falck, and M. Greven, Phys. Rev. Lett. **71**, 1621 (1993).

[15] J. D. Perkins, R. J. Birgeneau, J. M. Graybeal, M. A. Kastner, and D. S. Kleinberg, Phys. Rev. B **58**, 9390 (1998).

[16] Seong Hoon Jung, Jooyeon Kim, E. J. Choi, Y. Sekio, T. Kimura, and J. Lorenzana, Phys. Rev. B **80**, 140516 (2009).

[17] J. Lorenzana and G. A. Sawatzky, Phys. Rev. Lett. **74**, 1867 (1995).

[18] J. Lorenzana and G. A. Sawatzky, Phys. Rev. B **52**, 9576 (1995).

[19] Xiang-Xin Bi, and Peter C. Eklund, Phys. Rev. Lett. **70**, 2625 (1993).

[20] O. F. Schirmer, phys. stat. sol. (c) **4**, 1179 (2007)

[21] David Emin, Phys. Rev. B **48**, 13691 (1993)

FIG. 1: Optical reflectance of LuF_2O_4 single crystal with dc-voltage V applied (= R(V)). R(V) is normalized by the reflectance without the dc-voltage (= R(0)). The sharp features at low frequency $\omega < 1000\text{cm}^{-1}$ are due to optical phonons.

FIG. 2: Optical reflectance of LuF_2O_4 in the Far-IR frequency region. (a) R(V)/R(0) with dc-voltage V applied up to 7 V (b) R(T)/R(0) with the sample temperature T increased up to 380 K without applying the dc-voltage. In both plots R(0) is the room-temperature reflectance measured at dc-V = 0. The arrow in (a) indicates the hump structure which is absent in (b).

FIG. 3: Absolute reflectivity of LuF_2O_4 calculated from R(V)/R(0) and R(T)/R(0). (a) Voltage-driven reflectivity R_{abs}(V) for $0 \leq V \leq 7$ V (b) Temperature-driven reflectivity R_{abs}(T) for 290 K $\leq$ T $\leq$ 380 K at V = 0. They are calculated from R(V)/R(0) and R(T)/R(0) respectively (see text). Insets show the expanded view of the hump-structure in (a) and its absence in (b).

FIG. 4: Optical conductivity $\sigma_1(\omega)$ of $LuFe_2O_4$. (a) V-driven change from V = 0 to V = 7 V (b) T-driven change from 290 K to 380 K. Insets show the expanded view of $\sigma_1(\omega)$ in the region of the hump.

FIG. 5: Difference spectrum of optical conductivity. (a) V-induced effect $\Delta\sigma_1(V) = \sigma_1(V) - \sigma_1(0)$. (b) T-induced effect $\Delta\sigma_1(T) = \sigma_1(T) - \sigma_1(0)$. (c) Net optical conductivity induced by the dc-electric field, $\Delta\sigma_1(E) = \Delta\sigma_1(V) - \Delta\sigma_1(T)$.

Fig. 1

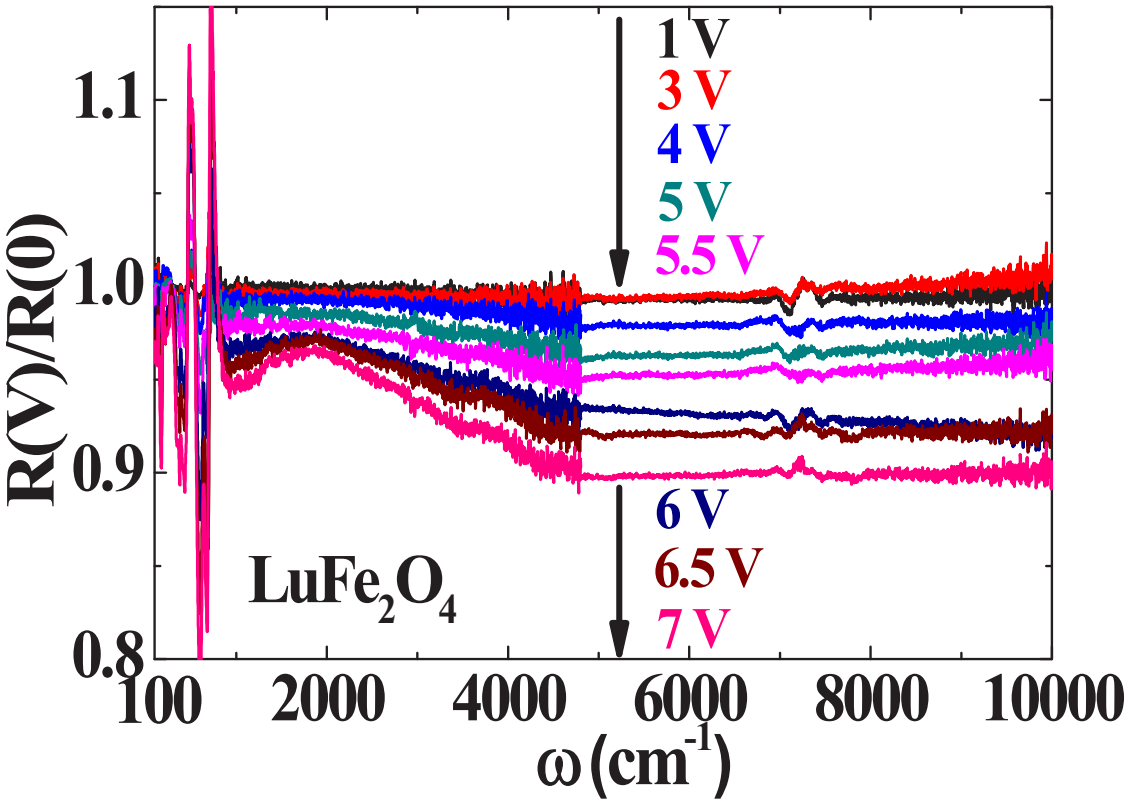

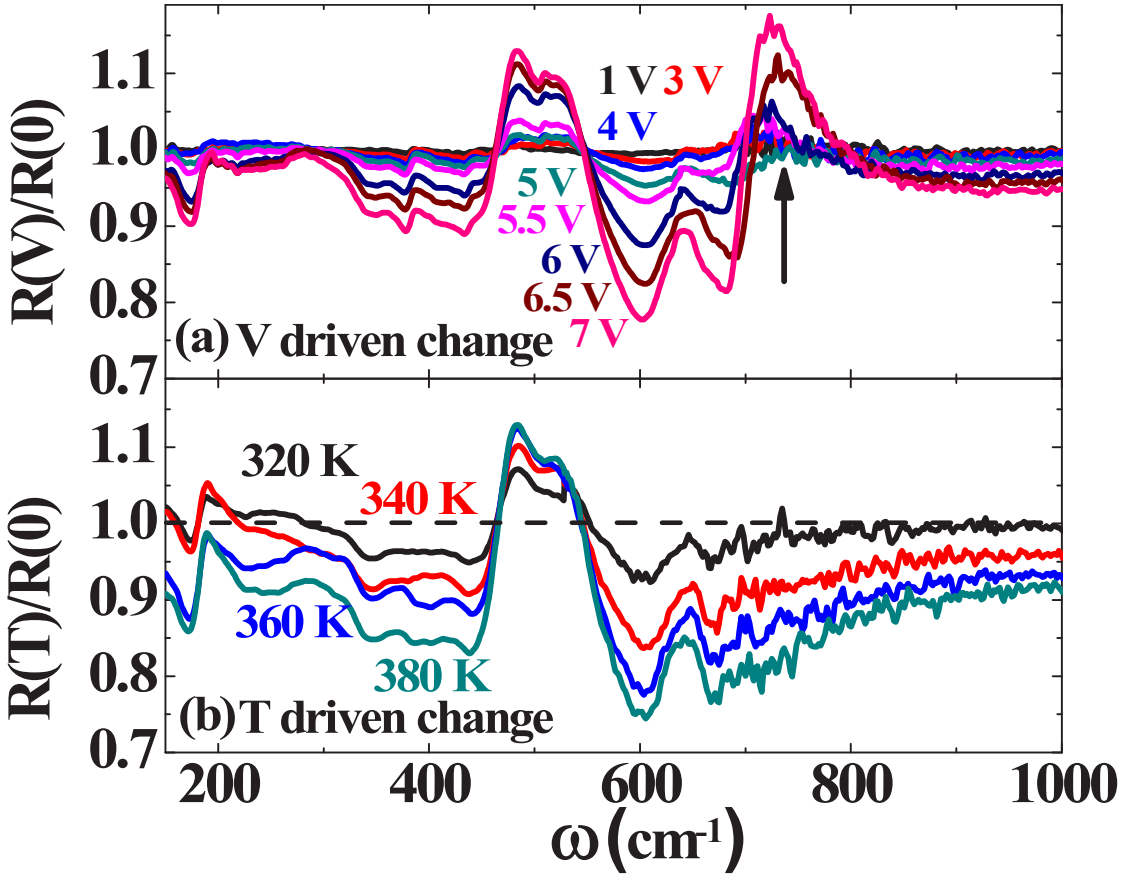
R(V)/R(0)
1.1
1.0
0.9
0.8
0.7
1 V
3 V
4 V
5 V
5.5 V
6 V
6.5 V
7 V
(a) V driven change
R(T)/R(0)
320 K
340 K
360 K
380 K
(b) T driven change
200
400
600
800
1000
ω (cm-1)

Fig. 2

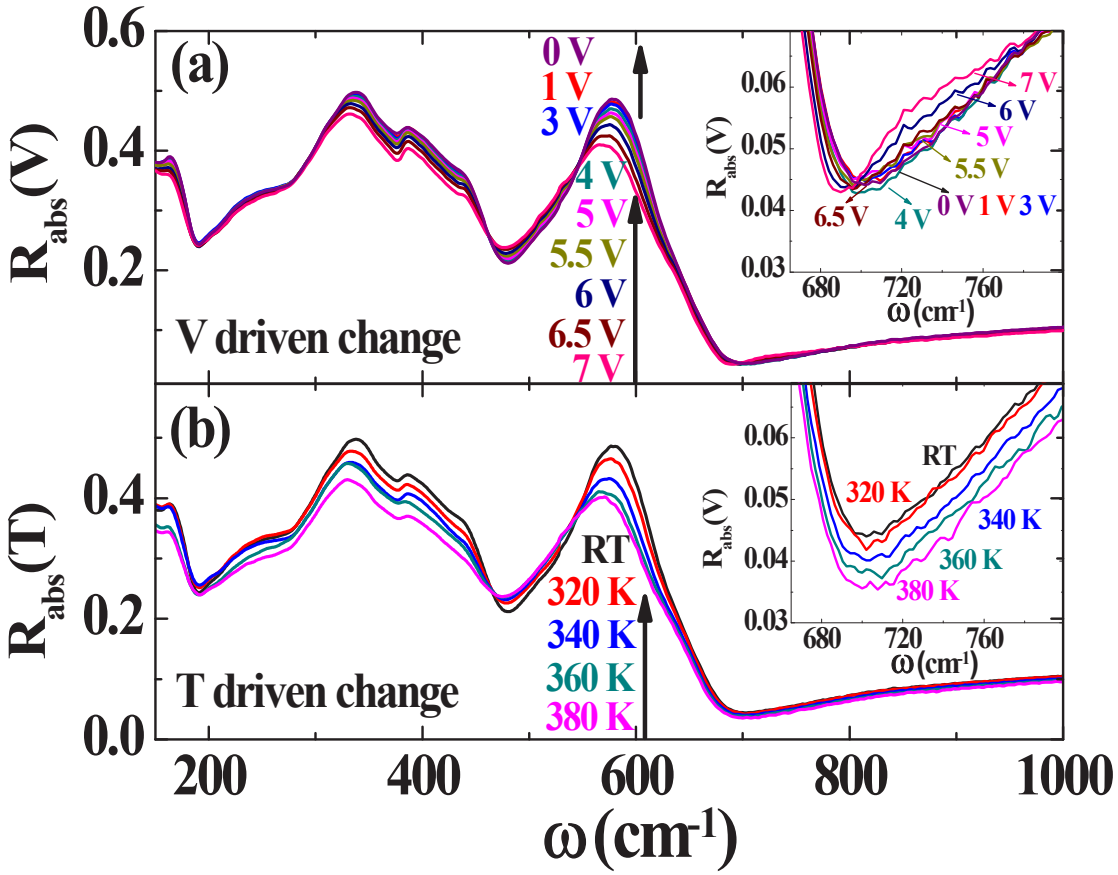
(a)
V driven change
0 V
1 V
3 V
4 V
5 V
5.5 V
6 V
6.5 V
7 V
R_abs(V)
(b)
T driven change
RT
320 K
340 K
360 K
380 K
R_abs(T)
ω(cm-1)

Fig. 3

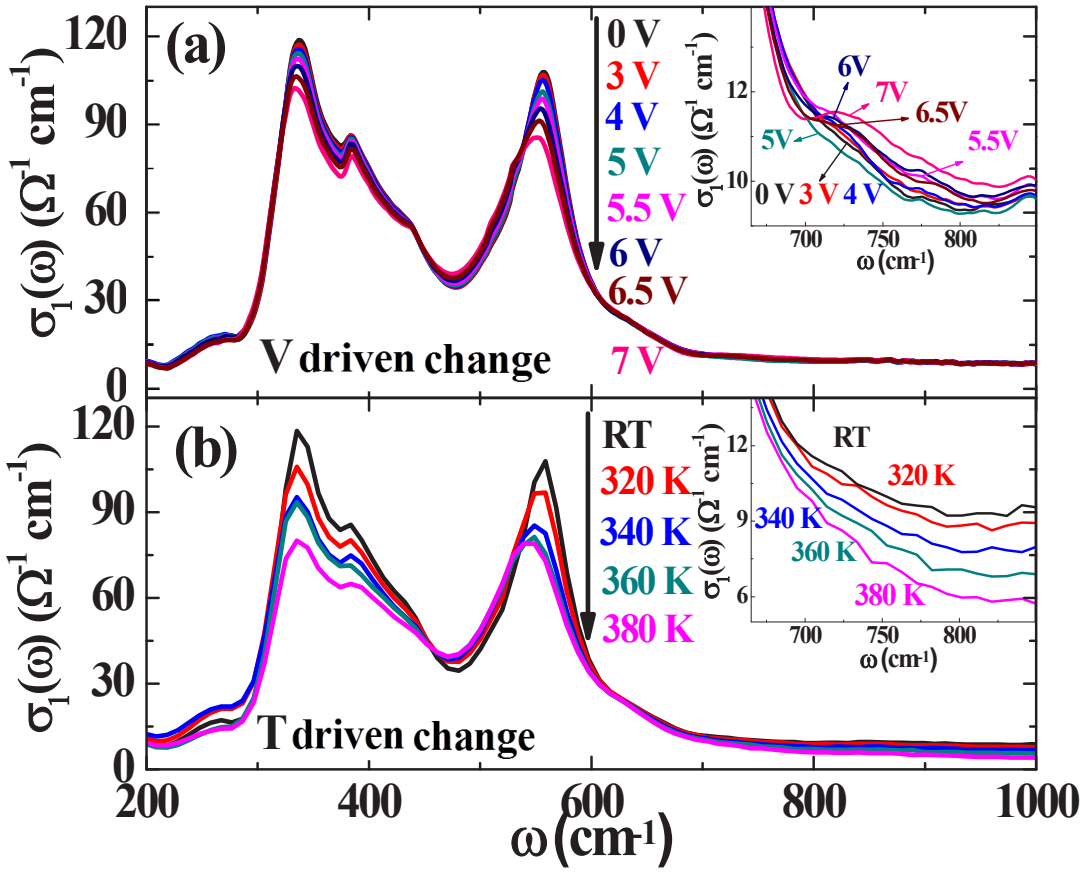
(a)
0 V
3 V
4 V
5 V
5.5 V
6 V
6.5 V
7 V
V driven change
6V
7V
6.5V
5V
5.5V
0 V 3 V 4 V
(b)
RT
320 K
340 K
360 K
380 K
T driven change
σ1(ω) (Ω-1 cm-1)
ω (cm-1)

Fig. 4

Fig. 5

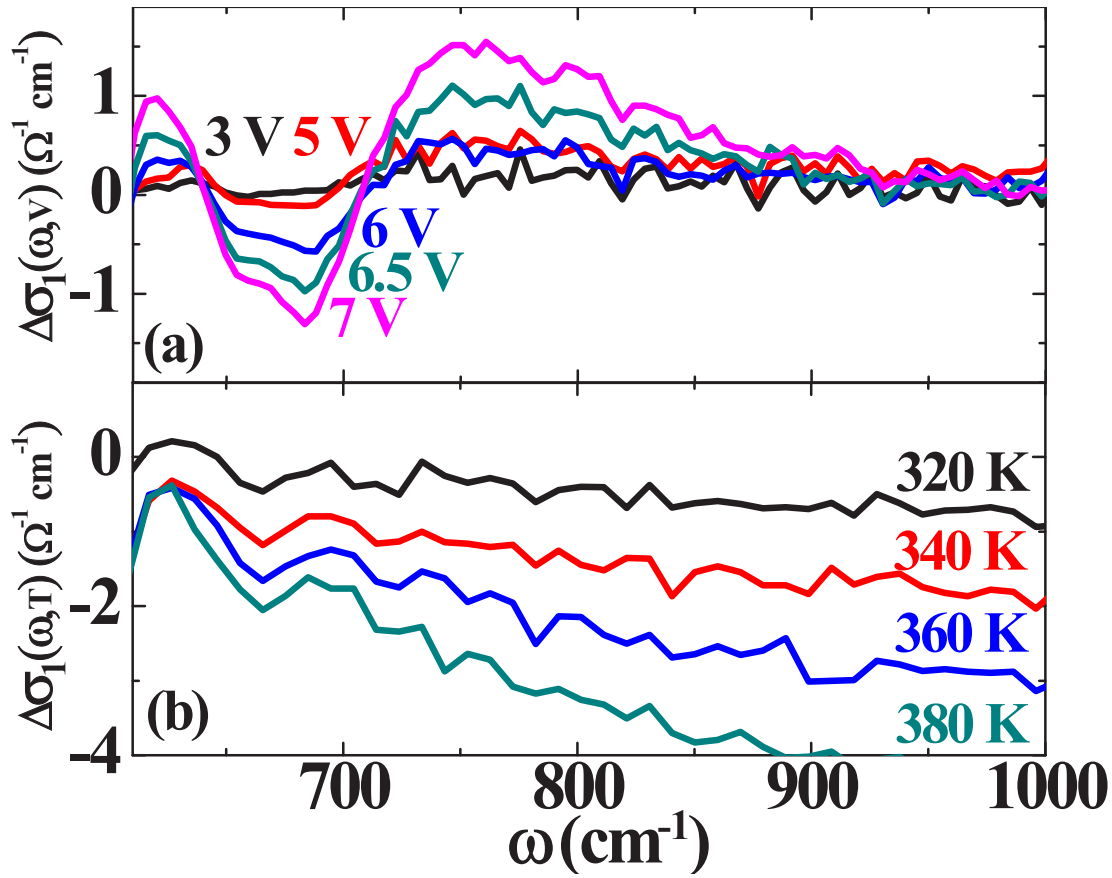
3 V
5 V
6 V
6.5 V
7 V
(a)
(b)
320 K
340 K
360 K
380 K
$\Delta\sigma_1(\omega,V)\ (\Omega^{-1}\ cm^{-1})$
$\Delta\sigma_1(\omega,T)\ (\Omega^{-1}\ cm^{-1})$
$\omega\ (cm^{-1})$

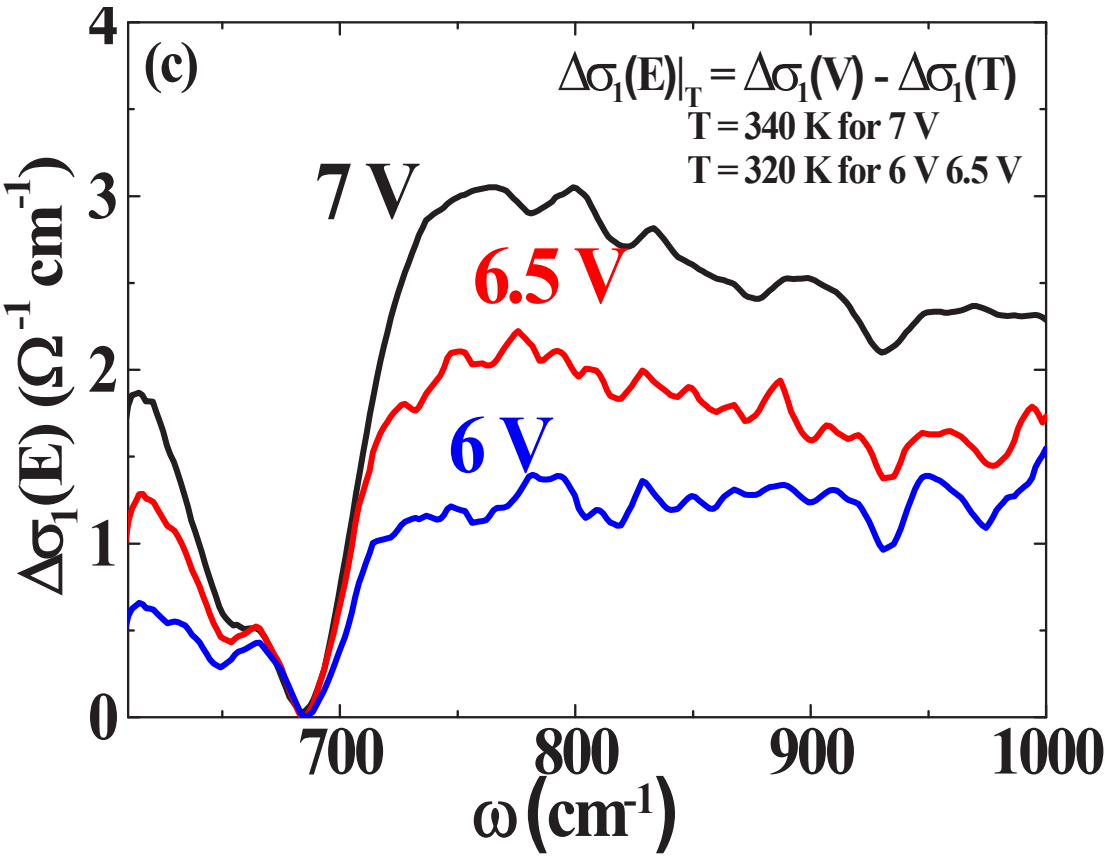
(c)
$\Delta\sigma_1(E)|_T = \Delta\sigma_1(V) - \Delta\sigma_1(T)$
T = 340 K for 7 V
T = 320 K for 6 V 6.5 V
7 V
6.5 V
6 V
$\Delta\sigma_1(E)\ (\Omega^{-1}\ cm^{-1})$
$\omega\ (cm^{-1})$